International Journal of Solids and Structures 108 (2017) 11–23

Contents lists available at ScienceDirect

International Journal of Solids and Structures

journal homepage: www.elsevier.com/locate/ijsolstr

Experimental and numerical assessment of the equivalent-orthotropic-thin-plate model for bending of corrugated panels

Yohko Aoki*, Waldemar Maysenhölder

Department of Acoustics, Fraunhofer Institute for Building Physics, Nobelstraße 12, 70569 Stuttgart, Germany

ARTICLE INFO

Article history:
Received 23 October 2015
Revised 27 July 2016
Available online 28 September 2016

Keywords:
Corrugated panel
Equivalent stiffness
Equivalent plate model
Orthotropic
Anisotropic
Sinusoid
Trapezoid
Bending
Vibration mode
Natural frequency

ABSTRACT

Numerous papers deal with the Equivalent Plate Model (EPM) for corrugated panels. Comparison of published formulas for the four relevant equivalent bending stiffnesses D_{11}^{eq}, D_{22}^{eq}, D_{66}^{eq}, andD_{12}^{eq} revealed ambiguities: Three different formulas were found for D_{22}^{eq}, which describes the bending of the ridges and troughs; for D_{66}^{eq} two 'competing' formulas emerged. Expressions not converging to the flat-plate values in the limit of vanishing corrugation height were discarded. All discussed formulas are written in a uniform notation for general one-dimensionally periodic shapes. Formulas derived for isotropic panel materials were generalized to the orthotropic case. In order to resolve the ambiguities and assess the EPM with regard to its range of applicability, vibration modes of six rectangular corrugated panels were measured. While agreement with numerical results obtained with COMSOL was fair, the EPM predictions of natural frequencies were satisfactory only for low-order modes. Finally, equivalent bending stiffnesses were determined numerically from COMSOL results for a few low-order modes by inverse methods. Thus the ambiguities with regard to D_{22}^{eq} and D_{66}^{eq} could be resolved. However, the D_{12}^{eq} values determined numerically came out significantly larger than the EPM prediction, in particular for stronger corrugations. Even though this discrepancy had little effect on the natural frequencies tested in the present paper, it remains a theoretical challenge.

1. Introduction

For a long time the bending of corrugated panels is conveniently described by a model in which the corrugated panel is replaced by an 'equivalent' flat homogeneous orthotropic thin plate. The bending properties of the corrugated panel are characterized and theoretically approximated by 'equivalent bending stiffnesses'. Numerous papers were published over the course of decades addressing various corrugation profiles like sinusoidal, trapezoidal or with circular segments. Different approaches have been used and partly differing results were obtained. It is not intended to provide a comprehensive literature review. Rather, a synopsis is presented in Section 2 with those results considered most relevant. They are 'translated' into a unique formulation for general one-dimensionally periodic shapes. Some explicit expressions for sinusoidal and trapezoidal shapes are given in the Appendix. Furthermore, derivations assuming isotropic panel materials were generalized to orthotropic panel materials. This literature evaluation ends up with undisputed expressions for two of the equivalent bending stiffnesses and with two or three differing expressions for the two remaining stiffnesses.

The Equivalent Plate Model (EPM) was assessed by studying the natural frequencies of free rectangular panels with sinusoidal or symmetric trapezoidal corrugation both experimentally and numerically using FEM. Section 3 presents results for three sinusoidal and three trapezoidal panels. The fair agreement between measured natural frequencies and FEM values indicates that (i) the experimental setup was close to the intentions and (ii) the FEM modeling using thin-shell elements was appropriate. Thus, these results can be considered a reasonable reference to judge the equivalent orthotropic-thin-plate model. The EPM predictions – the mentioned ambiguities are resolved in the following section – generally underestimate the reference values except for low-order modes.

In Section 4 two inverse methods for obtaining equivalent stiffnesses from measured or calculated vibration modes are applied to generate stiffness values for comparison with the EPM expressions. Naturally, with the results of Section 3 in mind, low-order modes were used. In this way convincing agreement was

* Corresponding author.
E-mail addresses: yohko.aoki@ibp.fraunhofer.de (Y. Aoki), maysenhoelder@ibp.fraunhofer.de (W. Maysenhölder).

http://dx.doi.org/10.1016/j.ijsolstr.2016.07.042

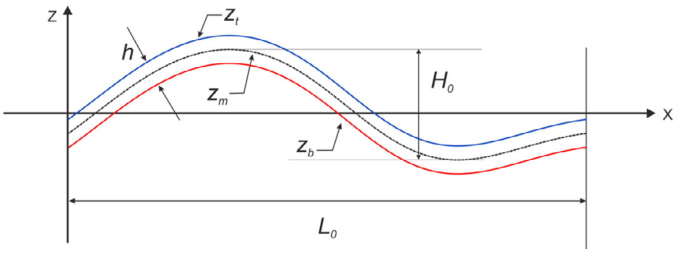

Fig. 1. Geometric description of corrugation profile. (See the web version of this article for all figures in color.)

obtained for three of the four equivalent stiffnesses, and the ambiguities could be removed. However, a significant discrepancy was observed in case of one of the equivalent stiffnesses. This is discussed in Section 5, which also summarizes the EPM formulas used in Section 3. Concluding remarks address the applicability from a somewhat more general perspective. A preliminary account of parts of the present work was presented at Forum Acusticum (Aoki and Maysenhölder, 2014).

2. Equivalent plate model (EPM)

2.1. Geometric corrugation description

Fig. 1 shows the cross-section of a unit cell of a singly curved periodic panel and the variables used for its geometric description. L_0 is the period. The x-axis runs across the ridges and troughs, while the y-axis runs along them. It is understood that the x-axis passes through the centroid of the unit cell and hence coincides with the neutral axis (Hansen, 1993). The corrugation profile is defined by the z-coordinate of the middle surface, z_m, as a function of x. The corrugation height, H_0, is taken as the difference between the maximum and minimum of z_m (Bartolozzi et al., 2014). It is assumed that the thickness of the panel, h, is everywhere the same. It is measured perpendicular to the middle surface giving rise to the bottom and top surfaces with z-coordinates z_b and z_t, which enclose the middle surface halfway in between. The difference $z_t(x)-z_b(x)$ is greater than or equal h; equality applies at positions x where the slope of z_m is zero (provided the height H_0 is not too big). More precisely, the outer surfaces may be defined – in the language of integral geometry – via Minkowski addition (Chiu et al., 2013) of the line $z_m(x)$ and a disk with radius $h/2$. This makes the definition unique also for shapes with sharp bends like trapezoidal ones.

An important quantity appearing in the formulas for the equivalent stiffnesses is the ratio of the arc-length of the middle-surface in one period, L_s, to the period L_0:

$$\frac{L_s}{L_0} = \frac{1}{L_0}\int_0^{L_0}\sqrt{1+\left(\frac{\mathrm{d}z_m}{\mathrm{d}x}\right)^2}\,\mathrm{d}x = \frac{1}{2\pi}\int_0^{2\pi}\sqrt{1+4\pi^2\left(\frac{H_0}{L_0}\right)^2\left(\frac{\mathrm{d}\zeta_m}{\mathrm{d}\varphi}\right)^2}\,\mathrm{d}\varphi \tag{1}$$

After the second equality sign normalized x- and z-coordinates have been introduced via $\varphi=2\pi\, x/L_0$ (with $z_m(\varphi)=z_m(x)$ understood) and $\zeta=z/H_0$. By this means it is immediately obvious that in the limit of infinite period L_0, with shape $\zeta_m(\varphi)$ and height H_0 kept constant, the ratio L_s/L_0 becomes unity. In the sequel this normalized representation will lead to compact expressions which facilitate the identification of dependencies and relations. The functions $z_b(x)$ and $z_t(x)$are in general rather complicated and cannot always be expressed explicitly (see Appendix).

Eq. (1) implies single-valued functions $z_m(x)$ or $\zeta_m(\varphi)$; this excludes re-entrant forms dealt with, e.g., by Kress and Winkler (2010). Similarly, $\zeta_b(\varphi)$ and $\zeta_t(\varphi)$ should be single-valued everywhere as well, i.e. the thickness h must be sufficiently small. Also, shapes like corrugated cylinders are not considered in this paper, which is confined to 'globally' flat panels and – in the examples – to symmetric shapes with a center of inversion at x_c and $z_m(-x+x_c)=-z_m(x-x_c)$, in particular sinusoidal and symmetric trapezoidal shapes.

2.2. Bending of orthotropic thin plates

For free vibration of orthotropic homogeneous thin (flat) plates the differential equation for the displacement w in the z-direction due to bending reads (Lekhnitskii, 1984, Section 91)

$$\mu\,\ddot{w} = D_{11}\frac{\partial^4 w}{\partial x^4} + 2(D_{12}+2D_{66})\frac{\partial^4 w}{\partial x^2\partial y^2} + 4D_{16}\frac{\partial^4 w}{\partial x^3\partial y} + 4D_{26}\frac{\partial^4 w}{\partial x\partial y^3} + D_{22}\frac{\partial^4 w}{\partial y^4} \tag{2}$$

with the areal mass density μ, the product of the density ρ and the thickness h. When the orthotropy axes are aligned with the x- and y-axes, D_{16} and D_{26} are equal to zero. The other four bending stiffnesses are given in terms of the material properties, Young's moduli E_{11} and E_{22}, Poisson's ratios ν_{12} and ν_{21}, and shear modulus G_{12} (Lekhnitskii, 1984, Section 61):

$$D_{11} = \frac{E_{11}}{1-\nu_{12}\nu_{21}}I, \quad D_{22} = \frac{E_{22}}{1-\nu_{12}\nu_{21}}I, \quad D_{12} = \nu_{12}D_{22} = \nu_{21}D_{11}, \quad D_{66} = G_{12}\,I, \tag{3}$$

where $I = h^3/12$ denotes the second moment of inertia per unit length. For infinite plates the combination $D_{12}+2D_{66}$ can be considered as a total torsional stiffness (Leissa, 1993, Section 9.2; Timoshenko and Woinowsky-Krieger, 1959, chapter 11, Eq. (212)-e). This implies that the number of independent elastic parameters reduces from nine in the orthotropic solid to three in the orthotropic thin plate. However, in boundary conditions, in particular in those involving free edges, D_{12} and D_{66} occur separately (Dickinson, 1978). Therefore all four stiffnesses D_{ij} of Eq. (3) have to be dealt with for an equivalent thin plate model which is applicable to finite corrugated panels, too. In the following this model is called Equivalent Plate Model and sometimes abbreviated by EPM (in the style of EFM for the Equivalent Fluid Model for fluid-filled porous structures).

Such a plate model should allow a reliable prediction of the 'global' behavior of the corrugated panel, be it infinite or finite, using an 'equivalent areal mass density' μ^{eq} and 'equivalent bending stiffnesses' D_{ij}^{eq}. For the sake of brevity and clarity these 'equivalent' quantities are normalized by their flat-plate analogs:

$$\hat{\mu}^{eq} = \frac{\mu^{eq}}{\mu}, \quad \hat{D}_{ij}^{eq} = \frac{D_{ij}^{eq}}{D_{ij}}. \tag{4}$$

Analytical determinations of the D_{ij}^{eq} which use the right-hand sides of Eq. (3) imply additional equivalent quantities (cf. Yokozeki et al., 2005; Isaksson et al., 2007; Bartolozzi et al., 2014):

$$\hat{E}_{ii}^{eq} = \frac{E_{ii}^{eq}}{E_{ii}}, \quad \hat{\nu}_{ij}^{eq} = \frac{\nu_{ij}^{eq}}{\nu_{ij}}, \quad \hat{G}_{12}^{eq} = \frac{G_{12}^{eq}}{G_{12}}, \quad \hat{I}^{eq} = \frac{I^{eq}}{I}. \tag{5}$$

Consequently,

$$\frac{\hat{D}_{12}^{eq}}{\hat{D}_{11}^{eq}} = \frac{D_{12}^{eq}}{\nu_{21}D_{11}^{eq}} = \frac{\nu_{21}^{eq}}{\nu_{21}} = \hat{\nu}_{21}^{eq}, \quad \frac{\hat{D}_{12}^{eq}}{\hat{D}_{22}^{eq}} = \hat{\nu}_{12}^{eq}. \tag{6}$$

One may even define a normalized equivalent thickness $\hat{h}^{eq} = h^{eq}/h$, which, with $I=h^3/12$ and $I^{eq}=(h^{eq})^3/12$, always results in $\hat{h}^{eq} = \sqrt[3]{\hat{I}^{eq}}$.